



VIRGINIA TECHTM



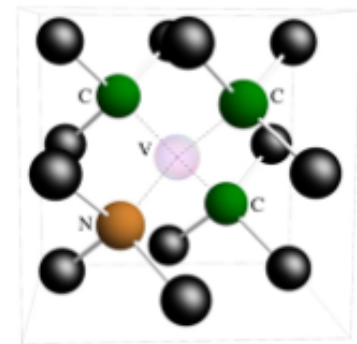
NV Center Defects in a Diamond Lattice

NICOLE BRAUNSCHEIDEL

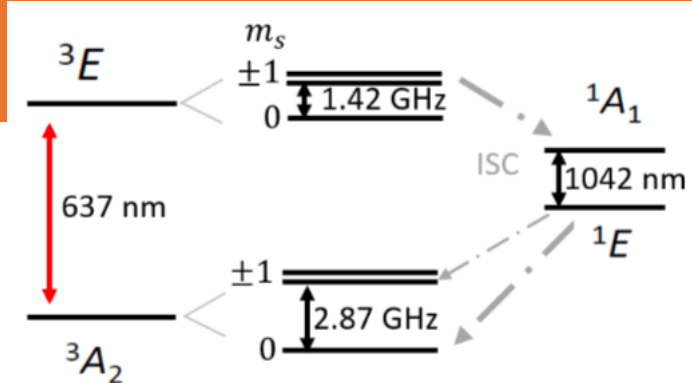
OCTOBER 1, 2020
GROUP MEETING

What are they?

- Wide-bandgap semiconductors
- Type Ib diamonds (diffuse, isolated nitrogen defects)
- Type Ila diamonds (absorb in a different region of IR spectra, different fluorescent characteristics)
- C_{3v} symmetry carbon lattice
- One carbon is deleted leaving 4 dangling bonds, one electron each
- Adjacent carbon is substituted with a nitrogen, introducing another electron
- Additional electron added to make NV⁻ center to have 6 electrons in the color center



Why study them?



- Qubit applications
- Triplet state allows for spin control ($^3A_2 \rightarrow ^3E$) from spin degrees of freedom
- Room temperature long coherence times
- Isotopic impurities that could result in nuclear-spin control
- Intersystem crossing (ISC) = Two-qubit gate possible
- Scalable to a multi-qubit register, coupling of NV center to NV center in lattice¹
- Caution: quantum info can leak out from the hyperfine interaction (ω_h) of the electronic spin with the environment (nuclear spins)

[1] Bernien, H.; Hensen, B.; Pfaff, W.; Koolstra, G.; Blok, M. S.; Robledo, L.; Taminiau, T. H.; Markham, M.; Twitchen, D. J.; Childress, L.; Hanson, R., Heralded entanglement between solid-state qubits separated by three metres. *Nature* **2013**, *497* (7447), 86-90.

Properties to study with *ab initio* methods

- Energy gaps/zero phonon lines (ZPL): what fluorescence experiments record
- Accurate electronic structure
- Molecular orbital diagrams
- Hyperfine couplings/nuclear spin control
- Coherence times
- Vibrational spectra
- Similar systems (SiV, divacancy, NV in silicon carbide)

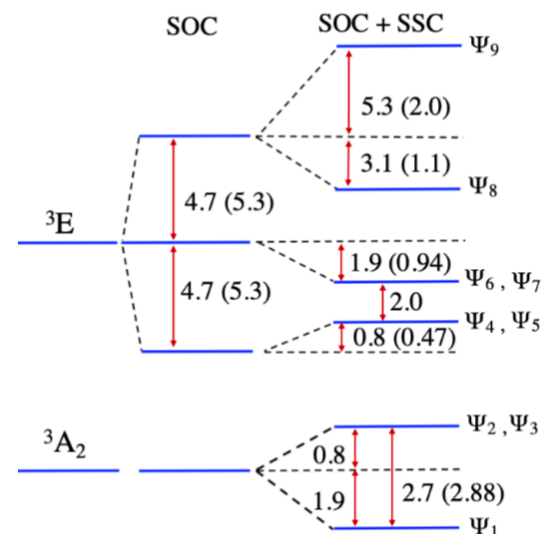
How to model them?

- DFT optimize structure
- Enforce the symmetry
- TD-DFT, MD, MP2, CIS, or CASSCF
- 4-6 electrons in 4-8 orbitals
- Spin-orbit coupling (SOC) splits 3E into angular spin states (in RASSI method)
- Spin-spin coupling (SSC) further splits 3E , but then also separates 3A_2 into the angular spin states

How to model them?

Table 4. Energy eigenvalues and eigenvectors for the ground- and first-excited triplet 3A_2 and 3E states calculated using the quantum chemistry methods including SOC and SSC. The energies are relative to the lowest SOC-included energy of each triplet state (3A_2 or 3E), as listed in Table 3 and shown in Fig. 5. Here $\Psi_{1,T}$, $\Psi_{2,T}$, and $\Psi_{3,T}$ are our calculated eigenstates (without SOC and SSC) listed in Table 2.

State		Energy (GHz)	Total wave function
3A_2	Ψ_1	-1.6	$\Psi_{1,T} S = 1, M_z = 0\rangle$
	Ψ_2	0.8	$\frac{1}{\sqrt{2}} (\Psi_{1,T} (S = 1, M_z = 1\rangle + S = 1, M_z = -1\rangle))$
	Ψ_3	0.8	$\frac{1}{\sqrt{2}} (\Psi_{1,T} (- S = 1, M_z = 1\rangle + S = 1, M_z = -1\rangle))$
3E	Ψ_4	0.9	$\frac{1}{\sqrt{2}} (\Psi_{2,T} + i\Psi_{3,T}) S = 1, M_z = 1\rangle$
	Ψ_5	0.9	$\frac{1}{\sqrt{2}} (\Psi_{2,T} - i\Psi_{3,T}) S = 1, M_z = -1\rangle$
	Ψ_6	2.9	$\Psi_{2,T} S = 1, M_z = 0\rangle$
	Ψ_7	2.9	$\Psi_{3,T} S = 1, M_z = 0\rangle$
	Ψ_8	5.7	$\frac{1}{2} \Psi_{2,T} (S = 1, M_z = 1\rangle + S = 1, M_z = -1\rangle)$ $-i\frac{1}{2} \Psi_{3,T} (S = 1, M_z = 1\rangle - S = 1, M_z = -1\rangle)$
	Ψ_9	14.8	$-\frac{1}{2} \Psi_{2,T} (S = 1, M_z = 1\rangle - S = 1, M_z = -1\rangle)$ $+i\frac{1}{2} \Psi_{3,T} (S = 1, M_z = 1\rangle + S = 1, M_z = -1\rangle)$



Literature

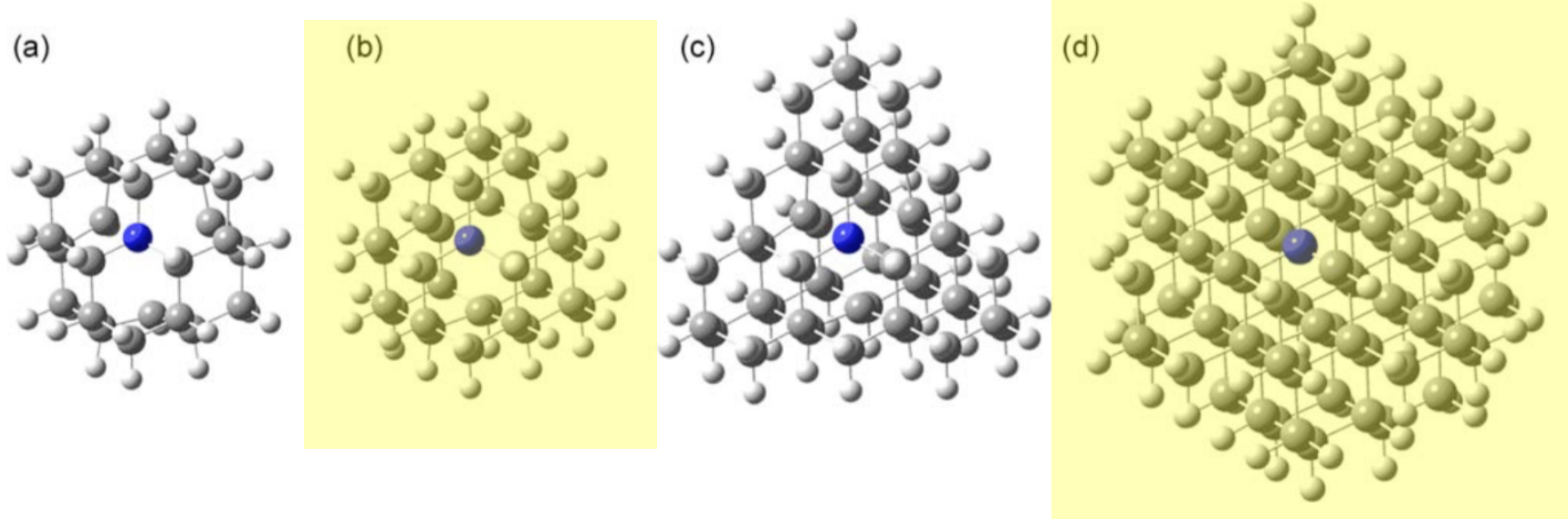
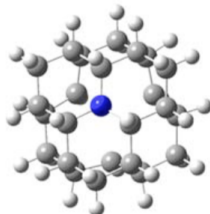


FIG. 1. (Color online) Several hydrogenated diamondoids containing $(NV)^-$ defect centers used in the calculations: (a) Disklike $C_{24}(NV)^-H_{30}$, (b) cuboidlike $C_{33}(NV)^-H_{36}$, (c) tetrahedron-like $C_{49}(NV)^-H_{52}$, and (d) sphere-like $C_{85}(NV)^-H_{76}$. In each model the nitrogen atom is located at the center, and the carbon cluster surface is passivated with hydrogen atoms.

Energy Gap

(a)

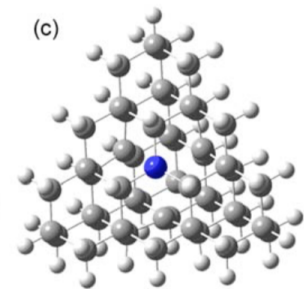


(b)

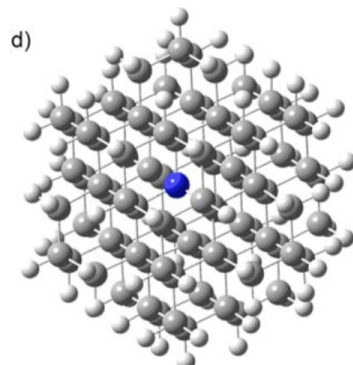


Species (conformation)	Method	Basis set	ΔE (eV)
C ₂₄ (NV) ⁻ H ₃₀ (disk)	TD-DFT	6-31G(d)	1.803
		6-31G(d) 6-31+G(d)	1.490
	CIS	6-31G(d)	2.115
		6-31G(d) 6-31+G(d)	1.316
	CAS(4,7)	6-31G(d)	2.553
		6-31G(d) 6-31+G(d)	2.521
	TD-DFT	6-31G(d)	1.737
		6-31G(d) 6-31+G(d)	1.556
C ₃₃ (NV) ⁻ H ₃₆ (cuboid)	CIS	6-31G(d)	2.106
		6-31G(d) 6-31+G(d)	1.778
	CAS(4,7)	6-31G(d)	2.532
		6-31G(d) 6-31+G(d)	2.480
	TD-DFT	6-31G(d)	1.913
		6-31G(d) 6-31+G(d)	1.739
	CIS	6-31G(d)	2.308
		6-31G(d) 6-31+G(d)	2.056
C ₄₉ (NV) ⁻ H ₅₂ (tetrahedron)	CAS(4,7)	6-31G(d)	2.587
		6-31G(d) 6-31+G(d)	2.577
	TD-DFT	6-31G(d)	1.761
		6-31G(d) 6-31+G(d)	1.566
	CIS	6-31G(d)	2.157
		6-31G(d) 6-31+G(d)	1.863
	TD-DFT	6-31G(d)	2.159
		6-31G(d) 6-31+G(d)	1.929
C ₈₅ (NV) ⁻ H ₇₆ (sphere)	CIS	6-31G(d)	2.649
		6-31G(d) 6-31+G(d)	2.640
	TD-DFT	6-31G(d)	2.161
		6-31G(d) 6-31+G(d)	2.054
	CIS	6-31G(d)	2.639
		6-31G(d) 6-31+G(d)	2.630
	TD-DFT	6-31G(d)	2.200
		6-31G(d) 6-31+G(d)	2.158
C ₁₀₄ (NV) ⁻ H ₈₆ (sphere)	CIS	6-31G(d)	2.681
		6-31G(d) 6-31+G(d)	2.670
	TD-DFT ^c	6-31G(d)	2.17 ± 0.02
		6-31G(d) 6-31+G(d)	2.66 ± 0.02
	CIS ^c	6-31G(d)	2.53 ± 0.03
		6-31G(d) 6-31+G(d)	2.18 ± 0.05
Average			
Expt. ^d			

(c)



(d)



Literature

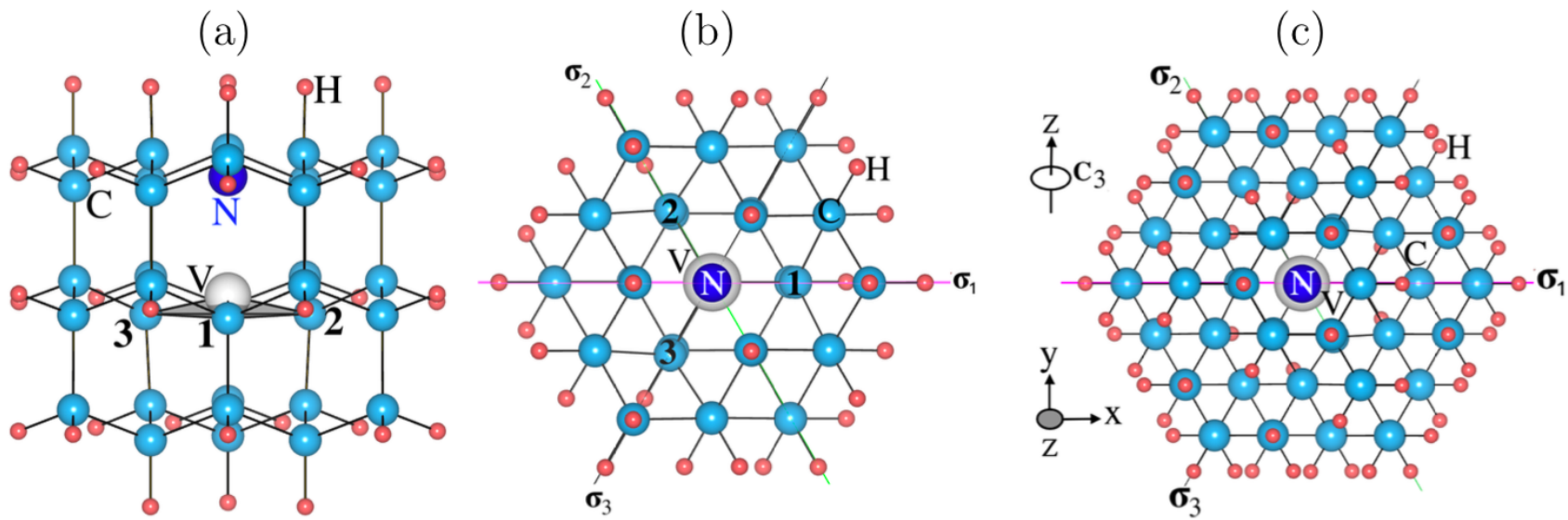


Figure 1. (a) Side view and (b) top view of the NV^- center defect in a 70-atom diamond cluster with C_{3v} symmetry. (c) Top view of the NV^- center defect in a 162-atom cluster with C_{3v} symmetry. The color scheme is as follows: carbon (cyan), nitrogen (blue), vacancy (grey), hydrogen (pink). Carbon, nitrogen, vacancy, and hydrogen are denoted by C, N, V, and H, respectively. The rotation axis of the three-fold symmetry (C_3) and the coordinate axes are shown. Here σ_1 , σ_2 , and σ_3 indicate vertical mirror planes passing through the carbons nearest to the vacancy with broken dangling bonds (labeled by 1, 2, and 3), the vacancy, and the z axis.

Energy Gap

Bhandari, C.; Wysocki, A.; Economou, S.; Dev, P.; Park, K. 2020

Reference \ Electronic State	3E	3A_1	3E	1E	1A_1	1A_2
Experiment [42, 31, 36]	1.945*[42] ~2.18[42]			0.33*-0.42* [36]	1.52*-1.61* [31]	
$C_{33}H_{36}N^-$ CASSCF(6,6) (This work)	1.93	2.95	3.06	0.34	1.41	3.23
$C_{85}H_{76}N^-$ CASSCF(6,6) (This work)	2.14	2.71	2.86	0.25	1.60	3.30
$C_{33}H_{36}N^-$ CASSCF(6,8)[41]	2.48					
$C_{49}H_{52}N^-$ CASSCF(6,8)[41]	2.57					
$C_{19}H_{28}N^-$ CASSCF(8,11)[40]	0.98		1.22	0.44	1.00	1.13(1E)
$C_{19}H_{28}N^-$ MRCI(8,10)[40]	1.36		1.61	0.50	1.23	1.37(1E)
$C_{42}H_{42}N^-$ MCCl[38]	1.96, 1.93			0.63, 0.64	2.06	
$GW+BSE$ [43]	2.32			0.40	0.99	2.25($^1E'$)
GW fit to model[44]	2.0*			~0.5	~1.5	~3.0($^1E'$)
	2.1					
CI-CRPA[19] (512-atom supercell)	1.75*			0.49	1.41	3.09($^1E'$)
Beyond-RPA [25] with quantum embedding theory	2.02					
$C_{33}H_{36}N^-$ DFT[60]	2.00			0.56	1.76	
DFT (512-atom supercell) [28]	1.77*			0.44	1.67	
	1.71*			0.9	0.0, 2.2	
$C_{42}H_{42}N^-$ DFT[38]	1.91					
	1.27			0.42	2.10	
$C_{284}H_{144}N^-$ DFT[38]	1.90				1.26($^1A'$)	
				0.48	2.03	
					1.26($^1A'$)	

Literature

TABLE 1. Vertical Excitation Energies ΔE_v of the NV⁻ Center.^a

symmetry	short wave function DFT/von Barth	Goss ⁸ DFT	Gali ⁹ DFT	C ₂₈₄ H ₁₄₄ N ⁻ DFT	C ₄₂ H ₄₂ N ⁻ DFT	C ₄₂ H ₄₂ N ⁻ CI	N _{CSF} CI
³ E _y ³ E _x	v \bar{x} \bar{y} \rangle v \bar{x} y \bar{y} \rangle		1.77	1.910	1.898	1.270	1.958 68669
¹ A ₁	(1/2 ^{1/2})[v \bar{v} x \bar{x} \rangle + v \bar{v} y \bar{y} \rangle]	1.67	≈0.0	2.028	2.096	2.060	1.932 73182
¹ A'	v \bar{v} x \bar{x} \rangle			1.255	1.259		83721
¹ E _y ¹ E _x	(1/2 ^{1/2})[v \bar{v} x \bar{y} \rangle - v \bar{v} \bar{x} y \rangle] (1/2 ^{1/2})[v \bar{v} y \bar{y} \rangle - v \bar{v} x \bar{x} \rangle]	0.44	≈0.9	0.482	0.422	0.629	88274
A''	v \bar{v} x \bar{y} \rangle v \bar{v} x \bar{y} \rangle	0	0	0.241	0.211	0	84376
³ A ₂				0	0	0	83434

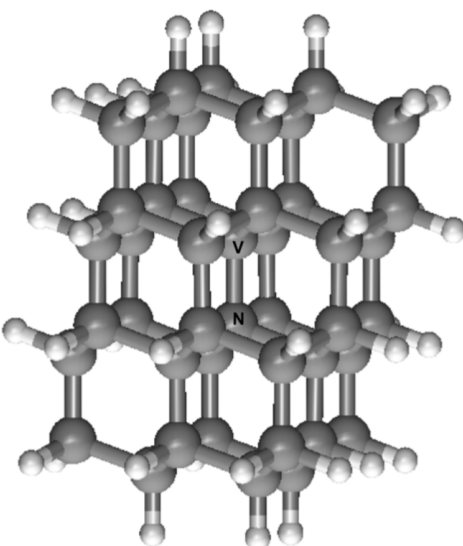


FIGURE 2. The C₄₄H₄₂ diamond cluster. C₄₂H₄₂N⁻ is built from it by removing the carbon atom marked V and replacing its neighbor marked N with a nitrogen atom.

Excited State Diagrams

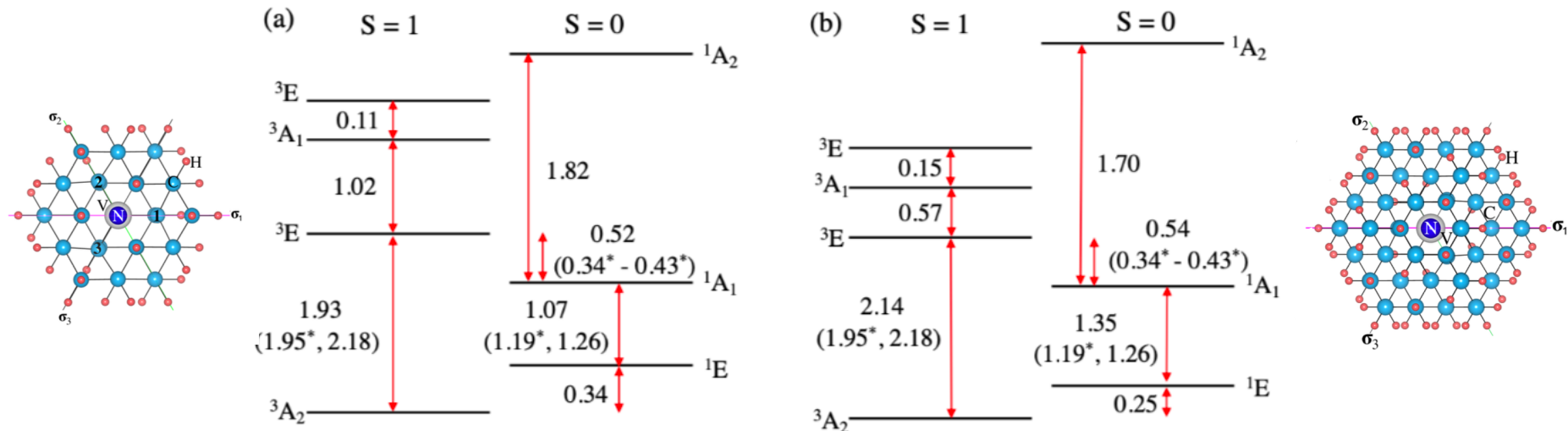
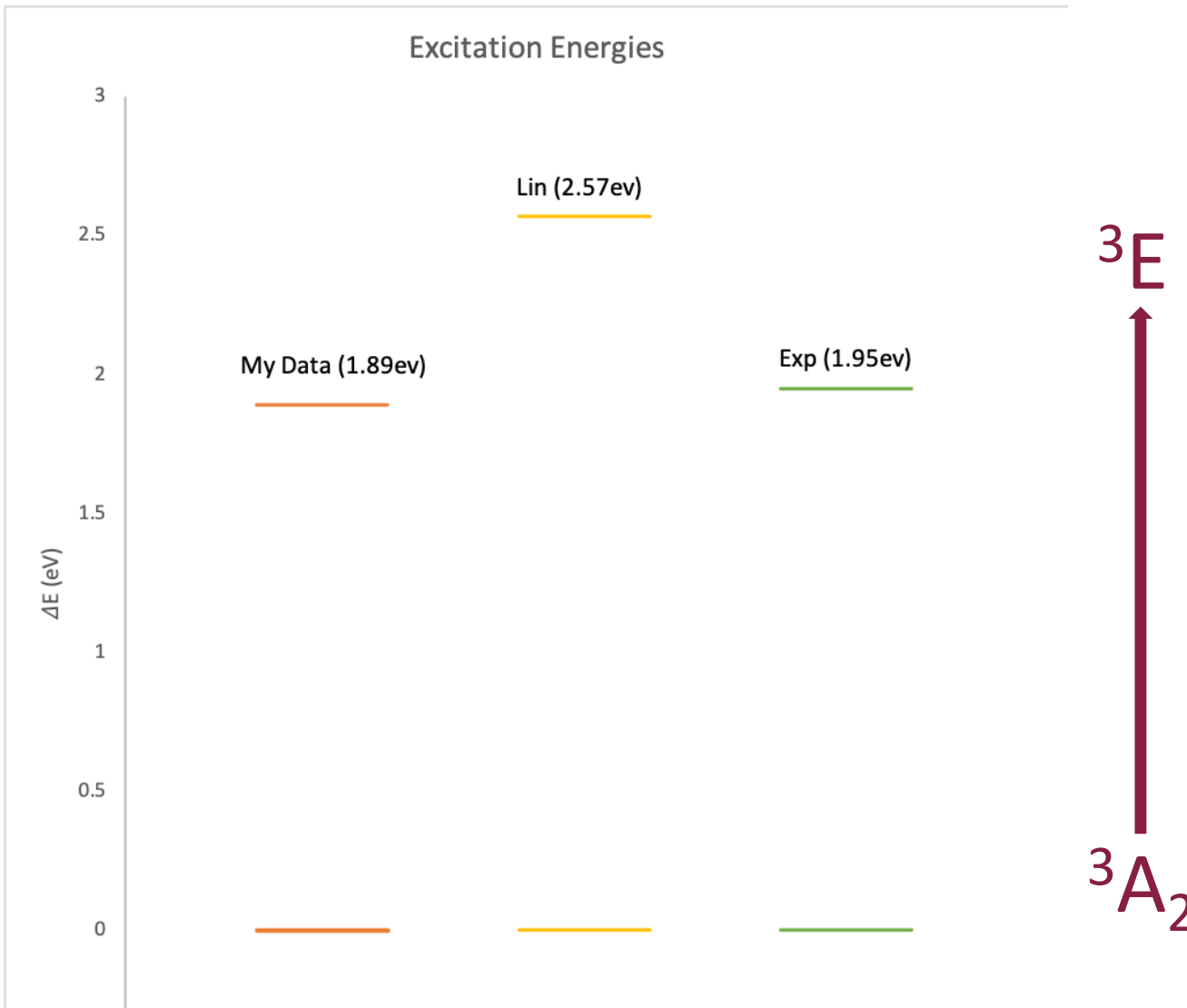
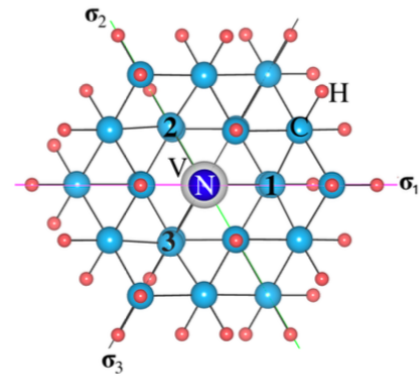


Figure 3. Schematic level diagrams of the spin-triplet and spin-singlet states for (a) the 70-atom and (b) the 162-atom diamond clusters obtained using the quantum-chemistry method without SOC or SSC. Here full electron correlation within the six molecular orbitals [Fig. 2(a) and (b)] are considered. The experimental zero-phonon absorption energies [31, 35–36, 42] and the experimental maximum-intensity peak energies of the phonon side band spectra (or experimental vertical excitation energies) are shown inside parentheses. The former energies are marked with *. All energy values are given in units of eV.

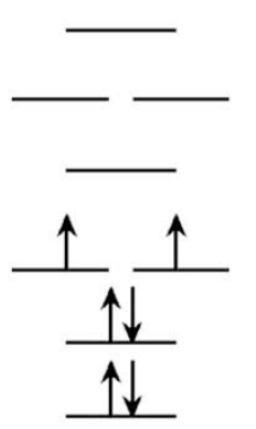
Energy Gap (ground-1st excited)



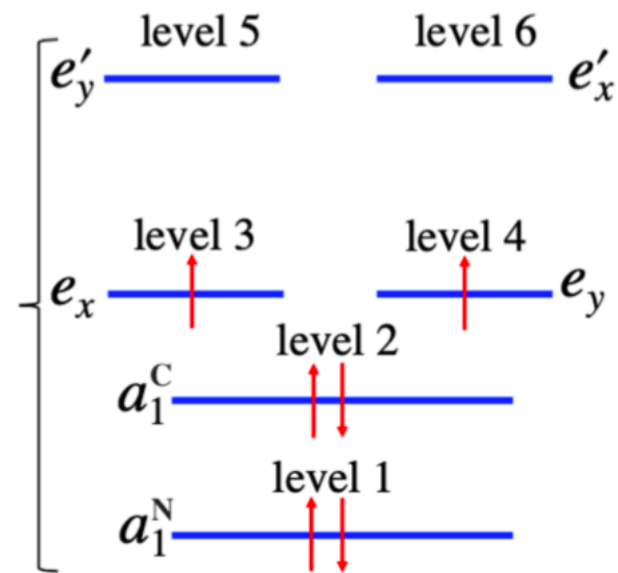
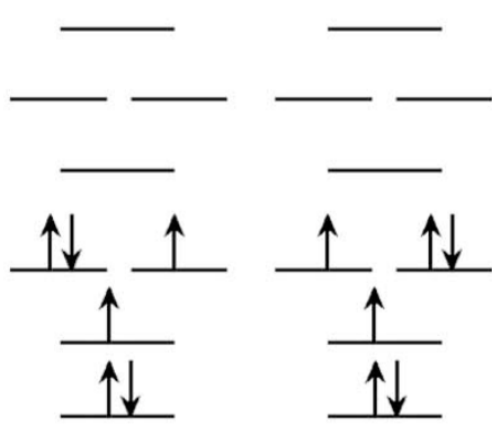
Electronic Structure/Active Space



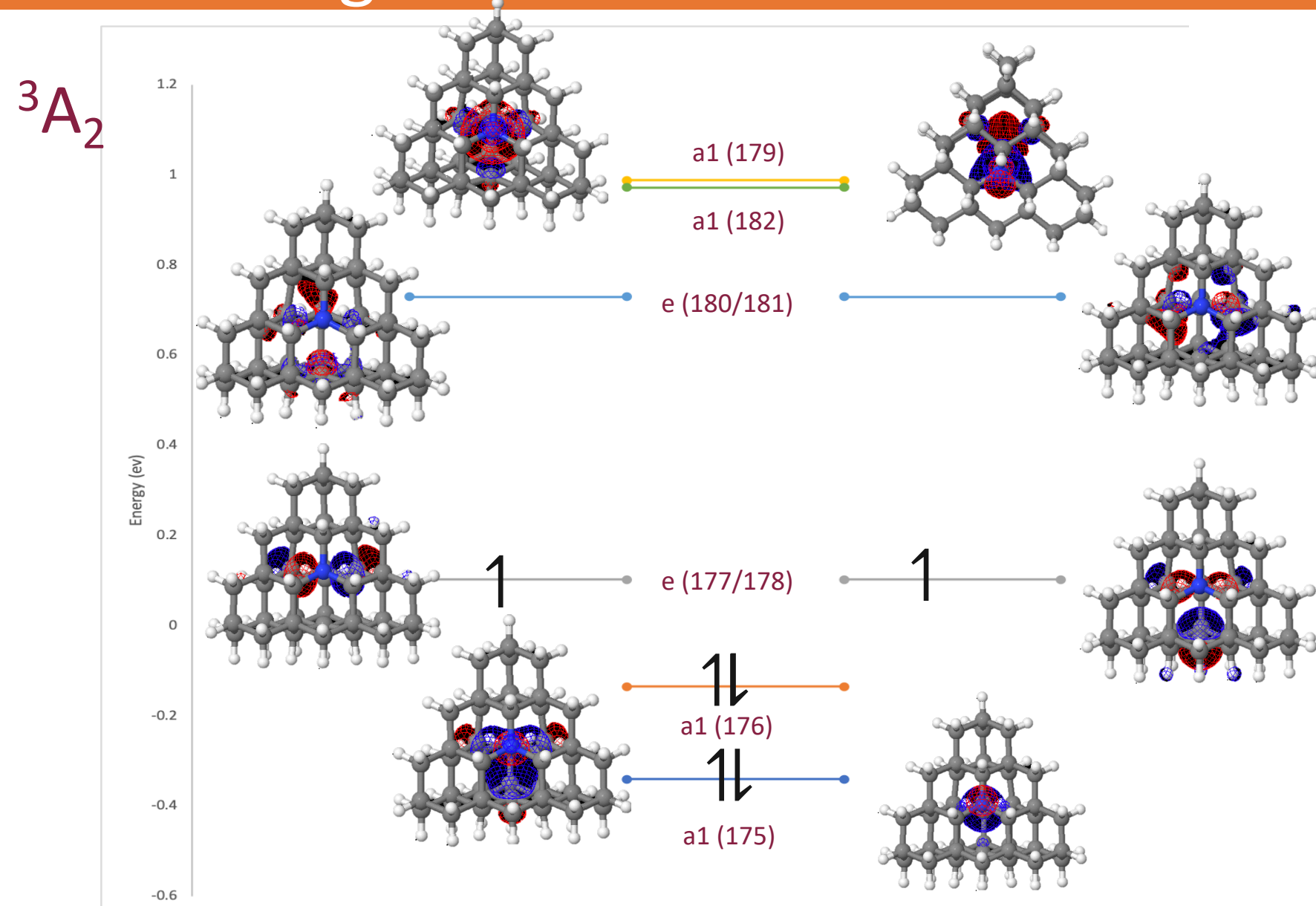
(a) Ground state, 3A_2



1st excited state, 3E



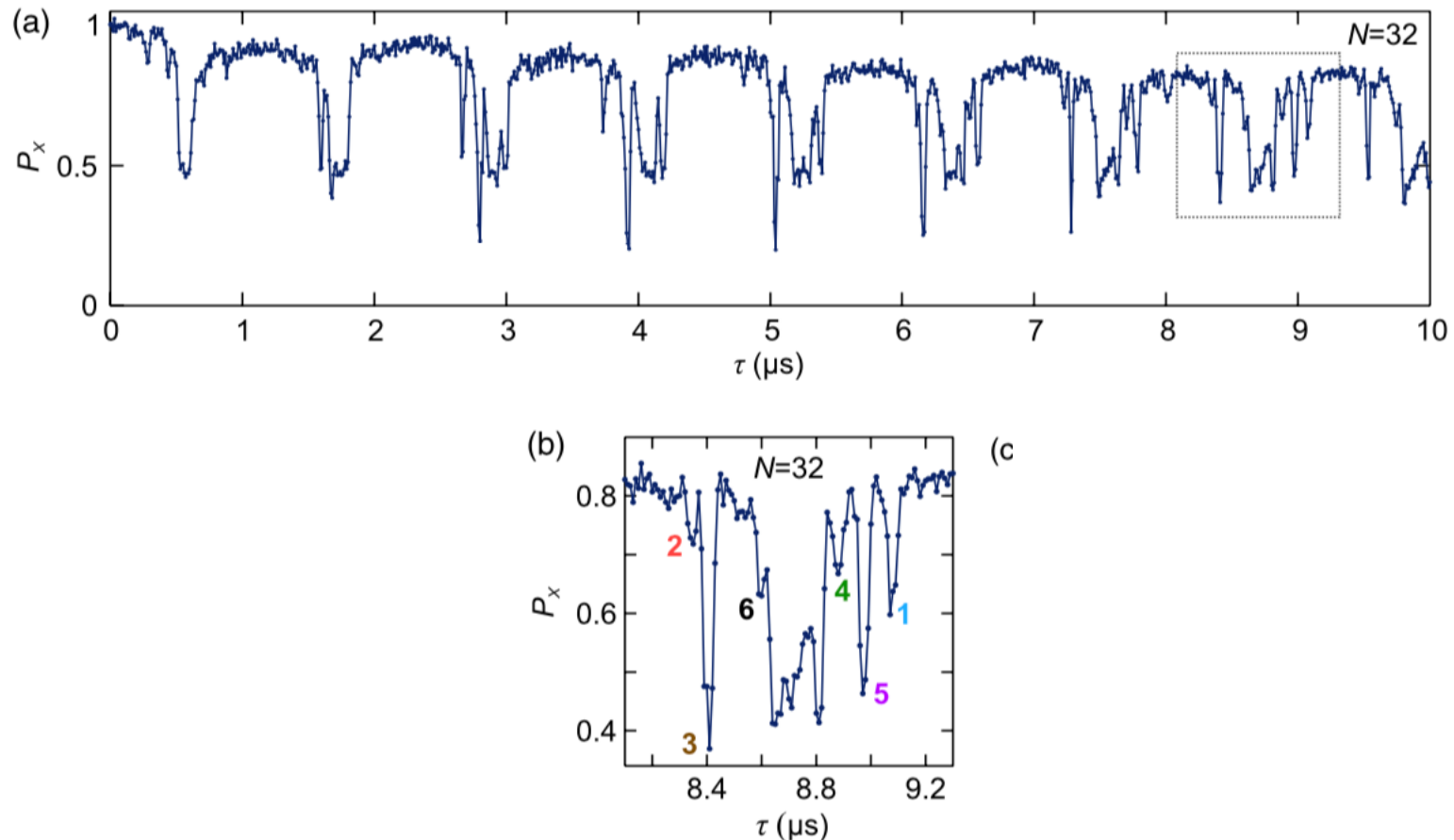
MO Diagram



Experimental control of nuclear spins

- Type IIa diamond
- Put NV center in $m_s = 0$ with laser and readout with spin-dependent fluorescence (if spin flips then no fluorescence)
- Use ESR and Ramsey measurements to see if there are any nearby strongly coupled ^{13}C spins
- Use decoupling sequence of π pulses with a τ parameter to dynamically decouple electron spin from other nuclei spins
- τ parameter can either:
 1. Decouple and conserve the NV spin
 2. Resonant with the ^{13}C spin, spike in signal and now entangled

Experimental control of nuclear spins



- P_x : probability to preserve the initial electron spin state after a decoupling sequence

Experimental control of nuclear spins

- Results in nuclear spin at an angle ϕ around an axis that is dependent on initial state of electron spin
- Can rotate the nuclear spin by tuning the number of pulses and τ
- Once you can identify, control, readout (single-shot, swapping with an electronic state etc.), you can have a controllable qubit!